LIDS-P -1249

September 1982

THE EFFECTS OF SMALL NOISE ON IMPLICITLY DEFINED NON-LINEAR DYNAMICAL SYSTEMS

by

Shankar Sastry*
Laboratory for Information and Decision Systems
Massachusetts Institute of Technology
Cambridge, MA 02139

*Research supported in part by the Air Force Office of Scientific Research under grant AFOSR-82-0258 . I would like to thank W.Fleming, H. Kushner, R. Landauer, S. Mitter, A. Willsky and J. Wyatt for several helpful discussions.

THE EFFECT OF SMALL NOISE ON IMPLICITLY DEFINED NON-LINEAR DYNAMICAL SYSTEMS

Abstract

The dynamics of a large class of non-linear systems are described implicitly, i.e. as a combination of algebraic and differential equations. These dynamics admit of jump behavior. We extend the deterministic theory to a stochastic theory since (i) the deterministic theory is restrictive, (ii) the macroscopic deterministic description of dynamics frequently arises from an aggregation of microscopically fluctuating dynamics and (iii) to robustify the deterministic theory. We compare the stochastic theory with the deterministic one in the limit that the intensity of the additive white noise tends to zero. We study the modelling issues involved in applying this stochastic theory to the study of the noise behavior of a multivibrator circuit, discuss the limitations of our methodology for certain classes of systems and present a modified approach for the analysis of sample functions of noisy non-linear circuits.

Keywords: Bifurcation, Singular Perturbation, Jump Behavior, Laplace's method, Noise behavior of non-linear circuits.

Section 1. Introduction

The dynamics of a large class of engineering systems are described only implicitly, for instance, those of non-linear circuits,swing dynamics of an interconnected power system, as also thermodynamic systems far from equilibrium. The implicit definition of their dynamics is as follows: the state variables are constrained to satisfy some algebraic equations, i.e. they are constrained to lie on a manifold M in the state space. The dynamics on this manifold M are then specified implicitly by specifying only the projection of the vector field on M onto a certain base space above which M lies. (i.e. a subspace of the original state space of the same dimension as M). The process of obtaining the system dynamics explicitly consists of 'lifting' the specified velocities onto a vector field on M (lifting is the inverse of projecting). Lifting may not, however, be possible at points where the projection map (restricted to the tangent space of the constraint manifold) has singularities. This singularity is typically resolved by regularization, i.e. by interpreting the algebraic constraint equations as the singularly perturbed limit of 'parasitic' or fast dynamics. The dynamics of the original system are obtained as the degenerate limit of the dynamics of the regularized system - the resulting trajectories may be discontinuous and this is referred to as jump behavior.

The foregoing deterministic theory needs to be extended to a stochastic theory for three reasons:

a) The conditions under which the limit trajectories to the regularizations exist are extremely restrictive so as to exclude several systems of interest.

b) Frequently, the algebraic constraint equations arise from the macroscopic aggregation of microscopically fluctuating dynamics, e.g. the flow of current in a resistor, the demand for electrical power at a distribution point in an electrical power network. More generally, deterministic equations describing thermodynamic systems are of this kind. Thus, the algebraic constraint equations contain in addition a rapidly fluctuating (or white noise) component.

c) The methods of analysis for deterministic systems of the implicitly defined kind involve techniques of bifurcation theory - their conclusions are extremely sensitive to imperfections and the addition of white noise.

Since in all the situations of interest to us, the intensity of the additive noise is small, we study in this paper the dynamics of implicitly defined dynamics in the presence of small additive noise. In fact, we compare the conclusions of the stochastic theory with those of the deterministic theory in the limit that the noise intensity tends to zero. The foregoing process requires the computation of two sets of limits: the limit that the regularization tends to zero and the limit that the intensity of the additive white noise tends to zero. In general, these limits do not commute. We explore in this paper the modelling issue of which sequence of limits is appropriate in the context of a specific system. The layout of the paper where we carry out this program is as follows:

In Section 2, we review briefly the dynamics of deterministic constrained systems and their jump behavior. With some minor modifications we follow here our earlier work [11] and the references contained therein.

In Section 3, we begin the study of noisy constrained dynamical systems. For the initial study we use as tools the work of Papanicolaou, et al [10] on martingale approaches to limit theorems. To study the

dynamics of noisy constrained systems in the presence of small noise, we develop and use in our context Laplace's method of steepest descent. We study in several separate cases, the comparison between the deterministic and small noise theory, describing: (i) how the stochastic theory yields conclusions about system dynamics when the deterministic theory fails and (ii) how the jump behavior of systems is modified by the presence of small noise. This section is a considerable extension of our previous work in the context of phase transitions in van der Vaals gases [12]. Several examples are presented to instantiate our results.

In Section 4, we present the detailed deterministic analysis of Section 2 applied to the dynamics of an emitter coupled relaxation oscillator circuit. We then show that the experimental conclusions of Abidi [1] on the dynamics of these circuits in the presence of small noise seem not to agree with the stochastic theory presented in Section 3.

In Section 5, we discuss the sequences of limits implied by the development of Section 3 - and the nature of systems for which this development yields the correct conclusions. In particular, we show that the development of Section 3 is relevant to systems where the separation in time scales between the slow and fast components is very large and is more important than the small intensity of the white noise (characterized by a certain sequence of limits subsumed by Section 3) - for instance in phase transitions, reaction rates and other phenomena of non-equilibrium thermodynamics. For non-linear circuits, however, the separation in time scales is less marked, so that we present here the relevant analysis (sample function calculations) for these systems with the order of limits reversed from that of Section 3. We use as tools the foundational

work of Ventsel-Freidlin [13] on small random perturbations of dynamical systems. We indicate heuristically how these results explain the experimental conclusions of Section 4.

In Section 6, we collect suggestions for future work. The present paper clearly is only a beginning in examining several phenomenological and modelling problems associated with the dynamics of constrained non-linear systems, such as non-linear circuits. It is our hope that the present work will eventually help in formulating a theory of the phenomenological behavior of non-linear circuits in the presence of noise. This is a topic of great interest in the simulation of VLSI circuits, where noise will play a bigger role in the face of shrinking device size.

Section 2. Deterministic Constrained Dynamical Systems and their Jump Behavior

The dynamics of a large class of engineering systems, for example, dynamics of non-linear circuits, swing-dynamics of an interconnected power system are not specified explicitly, but rather in the following constrained or implicit form:

$$\dot{x} = f(x,y) \tag{2.1}$$

$$0 = g(x,y) \tag{2.2}$$

Here $x \in \mathbb{R}^n$, $y \in \mathbb{R}^m$, f and g are smooth maps from $\mathbb{R}^n \times \mathbb{R}^m$ into $\mathbb{R}^n$ and $\mathbb{R}^m$ respectively. The equations (2.1), (2.2) need to be interpreted. Assume that 0 is a regular value of g. We then interpret (2.1), (2.2) as describing implicitly a dynamical system on the n-dimensional manifold

$$M = \{(x,y) \mid g(x,y) = 0\}$$

The vector field $X(x,y)$ on M is defined by specifying its projection along the x-axis, namely

$$\pi X(x,y) = f(x,y)$$

where π is the projection map $(x,y) \to x$. Identify the target space to M at (x,y) with a real vector space $TM(x,y)$ of dimension n (the null space of the matrix $[D_1 g(x,y) \vdots D_2 g(x,y)] \in \mathbb{R}^{m \times (n+m)}$) with origin parallelly translated to (x,y). $X(x,y)$ then is (in coordinates) a vector belonging to $TM(x,y)$. At points (x,y) where the mxm matrix $D_2 g(x,y)$ is non-singular, it follows that

$$\pi TM(x,y) = \mathbb{R}^n$$

and $f(x,y)$ uniquely specifies $X(x,y)$. Difficulties, however, arise at

points (x,y) where $D_2g(x,y)$ is not of full rank and $f(x,y)$ is transverse to $\pi TM(x,y)$; see, for example, Figure 1.

Another way of explicating the difficulty encountered in interpreting (2.1), (2.2) is as follows: Equation (2.2) is an algebraic equation which requires to be solved for y locally as a smooth function of x -- this is then substituted in equation (2.1) to yield the x trajectory. The y-trajectory may then also be obtained by

$$\dot{y} = -[D_2g(x,y)]^{-1} D_1g(x,y)\dot{x} \tag{2.3}$$

provided $D_2g(x,y)$ is non-singular). At points, where $D_2g(x,y)$ is singular; the implicit function theorem can no longer be invoked to solve equation (2.2) (locally) for y as a smooth function of x. Besides, equation (2.3) has an infinite right hand side so that the procedure suggested above for obtaining the trajectories of the system breaks down.

The fact that $\dot{y}$ becomes infinite at points (x_o,y_o) where $D_2g(x_o,y_o)$ is singular (hence forward referred to as singular points) leads us to suspect that a modified solution concept would require the integration of (2.1), (2.2) to be restarted from a non-singular point (x_o,y_1) belonging to M, after a jump (zero time transition) in the y-coordinate. Since we do not wish to choose the new start point of integration (x_o,y_1) in ad-hoc fashion we give a physically meaningful way of obtaining it, using the notions of singular perturbations:

In several practical problems, the algebraic equation (2.2) is in fact the degenerate limit as $\varepsilon \downarrow 0$ of

$$\varepsilon\dot{y} = g(x,y) \tag{2.4}$$

where $\varepsilon > 0$ is a small parameter representing parasitics neglected in the

course of modelling. Trajectories of (2.1), (2.2) are then interpreted to be the limit as $\varepsilon \downarrow 0$ of those of the well defined system (2.1), (2.4) (provided the limits exist).

A simple example of the application of this procedure is to the degenerate van der Pol oscillator described by

$$\dot{x} = y \tag{2.5}$$

$$0 = -x - y^3 + y \tag{2.6}$$

Figure 2 shows the phase portrait of the system (2.5), (2.6) with the zero equation (2.6) replaced by y. In the limit that $\varepsilon \downarrow 0$ the closed orbit of the non-degenerate system tends to a 'relaxation' oscillation including two jumps as shown in the figure.

The intuition for studying the augmented system is obtained by re-scaling (expanding) time t to $\tau = t/\varepsilon$ in equations (2.1), (2.4) and taking the formal limit that $\varepsilon \downarrow 0$:

$$\left.\begin{aligned} \frac{dx}{d\tau} &= 0 \qquad (2.7) \\ \frac{dy}{d\tau} &= g(x,y) \qquad (2.8) \end{aligned}\right\} S$$

The configuration manifold M of the system (2.1), (2.2) is the set of equilibrium of the "sped-up" system S. Further, the set of stable-equilibria of this system S are the portions of the configuration manifold M which are attracting to the parasitic dynamics. Stability of the equilibrium of S in which x is "frozen"is of course determined by the eigenvalues of the linearization, i.e. the eigenvalues of $D_2 g(x,y)$. Further, when the equilibria are hyperbolic (no eigenvalues of $D_2 g(x,y)$ $j\omega$-axis) the domains of attraction of these equilibria are their stable invariant manifolds.

The intuitive picture that now emerges in the original t-timescale is as follows: For a hyperbolic equilibrium point (x_o,y_o) of the sped-up system S attach its stable manifold $S^{x_o}_{y_o}$ transversally to M. When the attached manifold $S^{x_o}_{y_o}$ is of dimension m, then disturbances and noise will not cause the "state" (x,y) of the system (2.1), (2.2) to be repelled from M. If, in fact, the attached manifold is of dimension < m, disturbances may cause the "state" (x,y) to be repelled from M and follow instantaneously the dynamics of the sped-up system S to a new ω-limit set of (2.8). By assuming that (2.8) has only finitely many equilibrium points as its collection of ω-limit sets for each x, we may guarantee that (x,y) will transit eventually to $(x,\tilde{y})$ where $\tilde{y}$ is a new equilibrium point of S. If the new equilibrium point $(x,\tilde{y})$ is unstable it is likely that the 'state' will further change till a new stable equilibrium point is reached. In particular, this is the case when g(x,y) is the derivative with respect to y of a function $V : \mathbb{R}^{n+m} \to \mathbb{R}$ with finitely many critical points, i.e.

$$g(x,y) = D_2 V(x,y)^*$$

Other dynamical systems satisfying this assumption are referred to as gradient-like systems (see [11]. Note that the sped-up system S is not allowed to have closed orbits in its collection of ω-limit sets, by assumption.

Further, we assume that the only non-hyperbolic equilibrium points the system S has are those which have eigenvalues at the origin (rather than on the $j\omega$-axis), i.e. the only non-hyperbolic points are singular points. (This prevents the emergence of closed orbits by the Hopf bifurcation.) At these non-hyperbolic points, we study using techniques of bifurcation theory, the changes in the equilibrium behavior of S. Several possibilities

* $D_i^k V(x,y)$ is the k^{th} derivative of V with respect to the i^{th} argument (i=1,2).

arise -many equilibrium points coalesce and vanish (for instance in a fold bifurcation) or the equilibrium points change from being stable to being unstable (for instance in a cusp bifurcation). The fold and the cusp bifurcation are visualized in Figures 3 and 4, respectively, along with representative trajectories leading up to the non-hyperbolic or singular points. The determination of the specific kind of bifurcation behavior of $g(x,y)$ is possible using the techniques of Hale [4] and is illustrated in Sastry-Desoer [11].

Intuition, now, suggests that at the non-hyperbolic points, the state (x,y) finds itself in the domain of attraction of a new equilibrium point $(x,\tilde{y})$ of S and executes a jump to it. If this new point is unstable, another jump is permissible till a stable equilibrium point (x,y^*) of S is reached.

A great deal of the foregoing intuition can be made precise as shown in [10], and may be used to propose a solution concept for the sytem (2.1), (2.2) allowing for jumps from unstable hyperbolic equilibrium points of S and from singular equilibrium points of S .

However, it would appear from the foregoing brief discussion that the deterministic analysis of constrained systems is delicate and requires numerous assumptions on the sped-up system S . Further, the deterministic analysis does not yield a unique-solution concept at points (x_o,y_o) of S that have a stable manifold $S^{x_o}_{y_o}$ of dimension $< m$. It would appear then that a probabilistic analysis yielding probabilities of jump, and probabilities of the state lying at certain equilibria of the sped-up system rather than S would yield a more satisfactory solution concept to our constrained system. This, then, is the topic of our next section.

Section 3. Noisy Constrained Dynamical Systems

In the context of several applications, the presence of random fluctuations (which are of very high bandwidth - almost white), prompts us to write a more accurate model than that of the previous section, of the form

$$\dot{x} = f(x,y) + \sqrt{\mu}\,\xi(t) \tag{3.1}$$

$$\varepsilon\dot{y} = g(x,y) + \sqrt{\lambda\,\varepsilon}\,\eta(t) \tag{3.2}$$

Here, $\xi(\cdot)$ and $\eta(\cdot)$ are independent $\mathbb{R}^n$ valued and $\mathbb{R}^m$ valued white noise processes and λ,μ scale their variance. Equations (3.1), (3.2) differ from (2.1) and (2.4) in that they both contain additive, non-state dependent additive white noise terms. Note the $\sqrt{\varepsilon}$ scaling the variance of the white noise in equation (3.1). This is introduced, so that the sped-up system S (with ε then set equal to zero) in the time scale $\tau = t/\varepsilon$, is meaningful; namely

$$\frac{dx}{d\tau} = 0 \tag{3.3}$$

$$\frac{dy}{d\tau} = g(x,y) + \sqrt{\lambda}\,\eta(\tau) \tag{3.4}$$

For each $\varepsilon,\lambda,\mu > 0$ the evolution of the probability density $p^{\lambda}_{\mu,\varepsilon}(x,y)$ is governed by the forward-equation of Kolmogorov (or Fokker Planck equation)

$$\frac{\partial}{\partial t}\, p^{\lambda}_{\mu,\varepsilon} = (L_o^* + \frac{1}{\varepsilon} L_1^*)\, p^{\lambda}_{\mu,\varepsilon} \tag{3.5}$$

where L_o^* and L_1^* are formal adjoints of the operators L_o and L_1 given by

$$L_o p = \sum_{i=1}^{n} [\frac{\mu}{2} \frac{\partial^2}{\partial x_i^2} + f_i \frac{\partial}{\partial x_i}]p$$

and

$$L_1 p = \sum_{j=1}^{m} [\frac{\lambda}{2} \frac{\partial^2}{\partial y_j^2} + g_j \frac{\partial}{\partial y_j}]p \quad .$$

Proceeding, formally, from (3.5) we expect that in the limit that $\varepsilon \downarrow 0$ $p^{\lambda}_{\mu,\varepsilon}$ should satisfy

$$L_1^* \, p^{\lambda}_{\mu,o} = 0 \tag{3.6}$$

It follows by inspection of equations (3.4) that any solution to this equation is (up to a multiplicative function of x), the invariant density of the diffusion of equation (3.4) of the sped-up system S with x frozen. Thus,

$$p^{\lambda}_{\mu,o}(x,y) = \tilde{p}^{\lambda}_{\mu}(x) \quad \bar{p}^{\lambda}(x,y) \tag{3.7}$$

where $\bar{p}^{\lambda}(x,y)$ is the invariant density of the diffusion of (3.4) with x frozen (assumed to exist). Note that $\bar{p}^{\lambda}(x,y)$ also has the interpretation of being the conditional density of y given x, in the limit that $\varepsilon \downarrow 0$. Now, use (3.7) in (3.5) and note that the operator L_o^* does not involve the y-variable. Integrate both sides of (3.5) with respect to the y-variable to obtain

$$\frac{\partial \tilde{p}^{\lambda}_{\mu}}{\partial t}(x) = \bar{L}_o \, \tilde{p}^{\lambda}_{\mu}(x) \tag{3.8}$$

where

$$\bar{L}_o \, p = \sum_{i=1}^{n} \left[\frac{\mu}{2} \frac{\partial^2}{\partial x_i^2} + (\bar{f}_{\lambda})_i \frac{\partial}{\partial x_i} \right] p$$

with $\bar{f}_{\lambda}(x)$ being $f(x,y)$ averaged (integrated) over the invariant density of y given x, i.e.

$$\bar{f}_{\lambda}(x) = \int_{\mathbb{R}^m} f(x,y) \, \bar{p}^{\lambda}(x,y) \, dy \tag{3.9}$$

The foregoing manipulators suggest that the intuition for studying (3.1), (3.2) in the limit that $\varepsilon \downarrow 0$, is similar to that involved in the

study of (2.1), (2.4) as $\varepsilon \downarrow 0$. Equilibria of S with x frozen are replaced by the invariant density of the y process of (3.4) given x; and the drift in x instead of being f(x,y) evaluated at a specific equilibrium of g(x,y) is f(x,y) averaged over the invariant density of y - given x.

Conditions for the existence of an invariant density of (3.4), given x are far less restrictive than the condition that g(x,y) be gradient like (i.e. have only equilibrium points as its ω-limit sets) - see for example Bhattachanrya[2] or Papanicolaou, et al. [10]. Further, the foregoing formal manipulations can be made rigorous using Martingale methods and the following result has been obtained by Papanicolaou, et.al.[10]:

Theorem 3.1 [10] (Weak convergence for (3.1), (3.2)
Given any $T > 0$, the first component $t \to x(t)$ of the solution to (3.1), (3.2) converges weakly as $\varepsilon \downarrow 0$ in $C([0,T]; \mathbb{R}^n)$ to the unique diffusion $t \to x_{\lambda\,\mu}(t)$, governed by $\bar{L}_o$.

Remarks: (1) Weak convergence of a sequence of diffusions is convergence of their measures on $C([0,T]; \mathbb{R}^n)$ in the weak topology induced by endowing $C([0,T];\mathbb{R}^n)$ with the Skorokhod topology

(2) While it is true that the y-process of (3.1), (3.2) has no weak-convergent limit; the conditional density of y given x in the limit that $\varepsilon \downarrow 0$ is given by $\bar{P}^{\lambda}(x,y)$ of equation (3.7).

We now proceed to compare noisy-constrained systems with deterministic constrained systems:

3.1 Constrained Dynamical Systems in the Presence of Small Driving Noise

Frequently the model (3.1), (3.2) of noisy constrained systems differs from the deterministic model (2.1), (2.4) in only a small way - i.e. the variances μ,λ scaling ξ and η in equations (3.1) and (3.2) respectively are small. In the circuit context, as we shall show in the next section, μ and λ are of order of k T. (where k is the Boltzmann constant and T the temperature in degrees Kelvin), a quantity that is small at room temperatures. Thus, we compare the behavior of noisy constrained dynamical systems with that of the deterministic constrained systems of Section 2 in the limit that λ,μ the variances of the driving noise go to zero. The major tools used are Laplace's method of steepest descent for asymptotic calculations (see e.g. Chap. 4 of Hijab [5]), the techniques of Papanicolaou at al. [10], and the results of Ventsel-Freidlin [13]. The development is in several stages depending on the form of $g(x,y)$.

3.2 The Case of a Gradient Constraint Equation

Assume that $g(x,y)$ is the gradient with respect to y of a function $S(x,y)$, i.e.

$$g(x,y) = -\frac{1}{2}\,\mathrm{grad}_y\, S(x,y)$$

for some function $S : \mathbb{R}^n \times \mathbb{R}^m \to \mathbb{R}$. Then, the results of Papanicolaou, et al. [10] yield that provided the derivatives of S with respect to y grow rapidly enough at ∞ , the density of the diffusion generated by (3.4) converges exponentially to

$$\bar{p}^{\lambda}(x,y) = C^{\lambda}(x) \cdot \exp\left(-\frac{S(x,y)}{\lambda}\right) \tag{3.10}$$

where $C^{\lambda}(x)$ is chosen such that

$$\int_{\mathbb{R}^m} \bar{p}^{\lambda}(x,y)\,dy = 1$$

Note that for all $\lambda>0$ and $x \in \mathbb{R}^n$ the critical points (with respect to y of $\bar{p}^{\lambda}(x,y)$ are the equilibrium points of the deterministic system (2.4) with x frozen given in this instance by

$$\dot{y} = -\frac{1}{2} \operatorname{grad}_y S(x,y) \quad . \tag{3.11}$$

Further, if for some x_o, $S(x_o,y)$ is a Morse function (of y), then for all $\lambda > 0$ every local maximum of $\bar{p}^{\lambda}(x,y)$ is a stable equilibrium of (3.11).

To compare the noisy constrained system with the deterministic constrained system in the limit that $\lambda \downarrow 0$, it will be necessary to evaluate integrals like (3.9) in the limit that $\lambda \downarrow 0$. This is done using the following version of Laplace's method:

Theorem 3.2 (Laplace's Method)

Let for each $x \in \mathbb{R}^n$, $S(x,y)$ have global minima at $y_1^*(x)$, $y_2^*(x)$,...$y_N^*(x)$, where N may depend on x. Let them all be non-degenerate.† Further, let $S(x,y)$ have at least quadratic growth (in y) as $y \to \infty$. Then, in the limit that $\lambda \downarrow 0$, $\bar{p}^{\lambda}(x,y)$ converges to

$$\sum_{i=1}^{N} a_i(x)\ \delta(y - y_i^*) \Big/ \sum_{i=1}^{N} a_i(x)$$

where $a_i(x) = \det(D_2^2 S(x,y_i^*(x)))^{-1/2}$ (3.12)

More precisely, if $\phi(x,y)$ is a smooth function having polynomial growth as $y \to \infty$, then

$$\begin{aligned} \lim_{\lambda \downarrow 0} \bar{\phi}_{\lambda}(x) &= \lim_{\lambda \downarrow 0} \int_{\mathbb{R}^m} \phi(x,y)\ \bar{p}^{\lambda}(x,y)\,dy \\ &= \sum_{i=1}^{N} a_i(x)\ \phi(x,y_i^*(x)) \Big/ \sum_{i=1}^{N} a_i(x) \qquad (3.13) \\ &= \bar{\phi}_o(x) \end{aligned}$$

† i.e. the Hessian $D_2^2 S(x,y)$ at $y = y_i^*(x)$ is nonsingular

Proof: Since $\bar{p}^{\lambda}(x,y) = \exp - \frac{S(x,y)}{\lambda} \Big/ [\int_{\mathbb{R}^m} \exp - \frac{S(x,y)}{\lambda} dy]$,

we will first evaluate

$$\int_{\mathbb{R}^m} \phi(x,y) \exp - \frac{S(x,y)}{\lambda} dy$$

for simplicity first assume that $S(x,y)$ has a single global minimum at $\hat{y}$. We will then show that

$$\int_{\mathbb{R}^m} \phi(x,y) \exp - \frac{S(x,y)}{\lambda} dy = \phi(x,y^*) \frac{(2\pi\lambda^{m/2}) \exp - S(x,y^*)/\lambda [1 + o(1)]}{[\det D_2^2 S(x,y^*)]^{1/2}} \tag{3.14}$$

First, by the Morse Lemma (see for e.g. Milnor [16]) there exists a neighborhood U of $\hat{y}$ and a change of coordinates $\mathbb{R}^m \to U$ given by $y = \gamma(\bar{y})$ such that $y^* = \gamma(0)$ and

$$S(x,y) = S(x,y^*) + \frac{1}{2} \sum_{i=1}^{m} (\bar{y}_i)^2 \tag{3.15}$$

Further, outside the neighborhood U of y^*, $S(x,y) > S(x,y^*) + \delta$ for some $\delta > 0$ so that

$$\int_{\mathbb{R}^m/U} \phi(x,y) \exp - \frac{S(x,y)}{\lambda} dy = \exp[\frac{-S(x,y^*)}{\lambda}] \, o(\lambda^{\ell}) \tag{3.16}$$

for all $\ell > 0$. Clearly, then (3.16) does not contribute to the leading term of (3.14) Consider now

$$\int_U \phi(x,y) \exp - \frac{S(x,y)}{\lambda} dy = \exp - \frac{S(x,y^*)}{\lambda} \int_{\mathbb{R}^m} \exp (- \sum_{i=1}^{m} \bar{y}_i^2) \, \phi(x,\gamma(\bar{y})) \, |\det D\gamma(\bar{y})| \, d\bar{y} \tag{3.17}$$

Now, standard manipulations with Gaussian distributions yield that

$$\int_{\mathbb{R}^m} (\exp - \frac{1}{2\lambda} \sum_{i=1}^{m} y_i^{-2}) \, \phi(\bar{y}) \, d\bar{y}$$

$$= (2\pi\lambda)^{m/2} \, (\phi(0) + o(\lambda)) \tag{3.18}$$

Thus, to evaluate (3.17) we only need compute $|\det D\,\gamma(0)|$. Differentiating (3.15) twice with respect to y yields

$$D_2^2 \, S(x,y) = (\frac{d\bar{y}}{dy})^{-1})^T \, (\frac{d\bar{y}}{dy})^{-1} \quad . \tag{3.19}$$

From (3.19) it follows that

$$|\det D\,\gamma(0)| = [\det D_2^2 \, S(x,y^*)]^{-1/2}$$

so that (3.14) now is immediate on combining (3.16), (3.17) and (3.18)

In the instance that $S(x,y)$ has several global minima $y_1^*(x), y_2^*(x), \ldots, y_N^*(x)$ it follows from an easy extension of the foregoing argument that

$$\int_{\mathbb{R}^m} \phi(x,y) \exp - \frac{S(x,y)}{\lambda} dy = (2\pi\lambda)^{m/2} \exp \frac{-S(x,y^*)}{\lambda} [\sum_{i=1}^{N} \det [D_2^2 \, S(x,y_i^*(x))]^{-1/2}$$

$$\phi(x,y_i^*(x)) + o(1)] \tag{3.20}$$

Selling $\phi(x,y) = 1$ in (3.20) yields the corresponding expression for $\int_{\mathbb{R}^m} \exp \frac{-S(x,y)}{\lambda} dy$. Combining this with (3.20) we have equation (3.13).

□

Remarks: (1) If the growth conditions on $S(x,y)$ and $\phi(x,y)$ are uniform in x for $|x| \leq R$ it can be shown that for $p \geq 1$

$$\int_{|x| \leq R} |\bar{\phi}_\lambda(x) - \bar{\phi}_o(x)|^p \, dx \to 0 \quad \text{as } \lambda \downarrow 0 \tag{3.21}$$

The proof of (3.21) uses the dominated convergence and Egoroff's theorem.

(2) If $S(x,y)$ has a manifold M of global minima, then clearly these global minima cannot be non-degenerate. However, if $D_2^2 S(x,y)$ is non-degenerate in directions orthogonal to M, then a minor modification of the preceding theorem yields

$$\int_{\mathbb{R}^m} \exp\left[\frac{-S(x,y)}{\lambda}\right] \phi(x,y)\,dy = (2\pi\lambda)^{m/2}\, e^{\frac{-S(x,\hat{y})}{\lambda}} \left(\int_M \frac{\phi(x,y)}{H(x,y)} \cdot dy\Big|_M + o(1)\right) \tag{3.22}$$

Where $\hat{y}$ is any point belonging to M, $H^2(x,y)$ is the determinant of the non-degenerate part of the Hessian and $dy\Big|_M$ is the canonical measure on M.

We can now combine the results of Theorems (3.1) and (3.2) using a minor modification of the techniques of Papanicolaou, et. at. [10].

Theorem 3.3 (Weak convergence of (3.1), (3.2) as $\varepsilon,\lambda \downarrow 0$).

Given any $T > 0$, in the limit that $\varepsilon \downarrow 0$ and $\lambda \downarrow 0$ (in that order!), the first component $t \to x(t)$ of the solution to (3.1), (3.2) converges weakly in $C([0,T];\mathbb{R}^n)$ to the unique diffusion $t \to x_\mu(t)$ satisfying in law

$$\dot{x} = \bar{f}_o(x) + \sqrt{\mu}\,\xi(t) \tag{3.23}$$

where

$$\bar{f}_o(x) = \sum_{i=1}^{N} a_i(x)\, f(x,y_i^*(x)) \Big/ \sum_{i=1}^{N} a_i(x) \tag{3.24}$$

and the $y_1^*(x),\ldots,y_N^*(x)$ are the non-degenerate global minima of $S(x,\cdot)$ and $a_i(x) = [\det D_2^2 S(x,y_i^*(x))]^{-1/2}$.

Proof: Is presented in Sastry-Hijab [12].

Remark: The order of the limits is peculiar in Theorem (3.3). If the order is interchanged i.e. $\lambda \downarrow 0$ first and then $\varepsilon \downarrow 0$ it is clear that one recovers in the limit the deterministic development of Section 2 (with the minor modification that $\dot{x}$ has an additive white noise terms. The jump-behavior or the y-variable is as explained in that section. If, however, $\varepsilon \downarrow 0$ first and the $\lambda \downarrow 0$, the jump-behavior of the y-variable is somewhat different, as we now elaborate:

The behavior of the conditional density of y given x as $\lambda \downarrow 0$ is as in Theorem 3.2: the y variable is at one of the global minima of $S(x,\cdot)$ with probability proportional to the curvature of $S(x,)$ $((\text{Det } D_2^2 S(x,y_i^*))^{-1/2})$ at that minimum. Consider first the case when the minimum is unique. There is then a jump in the y-variable if there is a change in the global minimum of $S(x,\cdot)$ as x is varied. Points of jump then will be points of appearance and disappearance of global minima of $S(x,\cdot)$. This is in contrast to the deterministic picture of Section 2, where, for the instance that $g(x,y)$ is of the form of (3.11), stable equilibrium of the sped-up system S are local minima of $S(x,\cdot)$ and points of bifurcation are points appearance and disappearance of local minima of $S(x,\cdot)$.

We illustrate this with an example - the van der Pol oscillator of (2.5), (2.6) with added noise. Consider

$$\dot{x} = y + \sqrt{\mu}\,\xi(t)$$

$$\varepsilon y = -x - y^3 + y + \sqrt{\lambda\varepsilon}\,\eta(t)$$

Here $S(x,y) = -xy - \frac{y^4}{4} + \frac{y^2}{2}$ so that, in the limit that $\varepsilon \downarrow 0$; the x-process converges to one satisfying

$$\dot{x} = \overline{y}^{\lambda}(x) + \sqrt{\mu}\,\xi(t)$$

where

$$\overline{y}^{\lambda}(x) = \frac{\int_{-\infty}^{\infty} y \exp \frac{2}{\lambda}(-xy - \frac{y^4}{4} + \frac{y^2}{2})\, dy}{\int_{-\infty}^{\infty} \exp \frac{2}{\lambda}(-xy - \frac{y^4}{4} + \frac{y^2}{2})\, dy} ,$$

In the limit that $\lambda \downarrow 0$, the conditional density $\overline{p}^{\lambda}(x,y)$ converges to the delta functions shown in Figure 6. Note that the jump in the conditional density is from one leg of the curve $x = y - y^3$ to the other at $x = 0$, as contrasted with the deterministic behavior shown in Figure 2. $\overline{y}^{\lambda}(x)$ is plotted for different values of λ in Figure 7: and it mirrors this new jump behavior in y - the relaxation oscillation of Figure 2 no longer appears to exist.

It is possible to show exactly analogously to Theorems 3.1, 3.3 that in the limit that $\mu \downarrow 0$ the limit process of Theorem 3.3 given by (3.23) converges weakly on $C([0,T];\mathbb{R}^n)$ to the solution of the ordinary differential equation

$$\dot{x} = \overline{f}_o(x) \tag{3.25}$$

This, along with limit as $\lambda \downarrow 0$ of $\overline{p}^{\lambda}(x,y)$, completes the comparison of the noisy constrained systems with the deterministic constrained systems in the limit that the driving noise intensity goes to zero.

3.3 The Case of a Non-Gradientlike Constraint Equation

In this section we consider $g(x,y)$ of the form

$$g(x,y) = \frac{-1}{2} \operatorname{grad}_y S(x,y) + \psi(x,y) \tag{3.26}$$

where $\psi^T(x,y) \operatorname{grad}_y S(x,y) = 0$, i.e. a gradient constraint along with a term orthogonal to it. Such systems, in general, have closed orbits

as their ω- limit sets so that the deterministic development of Section 2 does not apply.

Proposition 3.4 (Invariant density for the system (3.26)

If the derivatives (with respect to y) of $S(x,y)$ go to ∞ sufficiently rapidly as $y \to \infty$; then the invariant density of the diffusion generated by

$$\dot{y} = \frac{-1}{2} \operatorname{grad}_y S(x,y) + \psi(x,y) + \sqrt{\lambda}\, \eta(t) \qquad y(0) = y_o$$

is given by

$$\bar{p}^{\lambda}(x,y) = [\exp - S(x,y)/\lambda] \Big/ \int_{\mathbb{R}^m} \exp - S(x,y)/\lambda \, dy \tag{3.27}$$

Proof: The existence of the invariant density is assured by Papanicolaou et.at. [10] and the form (3.27) is verified by substitution of (3.27) into equation (3.6), which it should satisfy, viz

$$\sum_{j=1}^{m} [\frac{\lambda}{2} \frac{\partial^2}{\partial y_j^2} - \frac{\partial}{\partial y_j} (-\frac{1}{2} \frac{\partial}{\partial y_j} S(x,y) + \psi_j(x,y)] \bar{p}^{\lambda}(x,y) = 0$$

The discussion and Theorem (3.2), (3.3) of Section (3.2) then apply to find the limit behavior of $\bar{p}^{\lambda}(x,y)$ and the x-component of the diffusion. Of special interest to us is the case when the deterministic system

$$\dot{y} = g(x,y) \tag{3.28}$$

has limit cycles, so that the deterministic theory of section 2 no longer applies. We begin with

Example 3.5 Consider with n = 1, m = 2 the system

$$\dot{x} = f(x,y_1,y_2) + \sqrt{\mu}\, \xi \tag{3.29}$$

$$\left.\begin{aligned} \varepsilon\dot{y}_1 &= y_2 + y_1(x^2 - y_1^2 - y_2^2) + \sqrt{\varepsilon\lambda}\,\eta_1 \\ \varepsilon\dot{y}_2 &= -y_1 + y_2(x^2 - y_1^2 - y_2^2) + \sqrt{\varepsilon\lambda}\,\eta_2 \end{aligned}\right\} \tag{3.30}$$

For this example

$$S(x,y) = -x^2(y_1^2 + y_2^2) + \left(\frac{y_1^4 + y_2^4}{2}\right) + y_1^2\, y_2^2 \tag{3.31}$$

and $\psi(x,y) = \begin{pmatrix} y_2 \\ -y_1 \end{pmatrix}$. By converting the system (3.28) for this example, into polar coordinates (viz. $r = \sqrt{y_1^2 + y_2^2}$, $\theta =$ arc tan y_2/y_1), it may be seen that the phase portrait of (3.28) has a stable, circular limit cycle in the y_1, y_2 plane of radius $|x|$ and an unstable equilibrium point at $\begin{pmatrix} 0 \\ 0 \end{pmatrix}$ except when $x = 0$ (in which case only a stable equilibrium point at $(0,0)^T$ exists). Thus, the deterministic theory of Section 2 is inapplicable. For the stochastic analysis note that the global minima of $S(x,y_1,y_2)$ given by (3.31) form a 1 dimensional manifold, P

$$\{(y_1,y_2) : y_1^2 + y_2^2 = x^2\} \quad .$$

Thus, the modified version of Theorem (3.2), given in remark (2) following the theorem and (3.22) needs to be invoked to obtain the limit as $\lambda \downarrow 0$ of the conditional density for y given x, $\bar{p}^{\lambda}(x,y)$. It is intuitive that as $\lambda \downarrow 0$, $\bar{p}^{\lambda}(x,y)$ converges to the uniform measure supported on the manifold P (see Figure 8). and that the averaged version of $f(x,y_1,y_2)$ over this measure may be written as

$$\bar{f}_o(x) = \int_0^{2\pi} f(x, |x|\cos\theta\ ,\ |x|\sin\theta)\,\frac{d\theta}{2\pi} \qquad \square$$

With $g(x,y)$ of the form specified by (3.26) it is easy to check that $S(x,y)$ is decreasing along the trajectories of (3.28). Hence, on any ω-limit set $S(x,y)$ is a constant. It is clear that if $S(x,y)$ has only

isolated critical points that (3.26) is a gradient-like system. However, if $S(x,y)$ has manifolds of critical points as in Example (2.5); its ω-limit sets could include closed orbits or even almost periodic motion on an invariant torus. In all of these cases the deterministic theory fails, but the stochastic theory utilizing remarks (2) after Theorem (3.2) yields a satisfactory resolution, with a well defined limit probability density $\bar{p}^{\lambda}(x,y)$ for y given x and a suitable averaging for the x-drift.

Remarks: (1) The calculations presented above enable us to conclude that in the limit that $\lambda \downarrow 0$, $\bar{p}^{\lambda}(x,y)$ picks out the "most-stable" features of the phase portrait of the deterministic system for the class of systems discussed in Section 3.2, 3.3.

(2) We have considered here only the case when the intensity of the driving noise in equations (3.1), (3.3) is state independent. The basic results of Section 3.1 continue to hold in the state dependent case, provided that the noise-intensity is nowhere degenerate. The conditional density $\bar{p}^{\lambda}(x,y)$ is seldom of the form studied in Sections 3.2, 3.3, however. We discuss this point further in the next section.

3.4 More General Constraint Equations

The stochastic differential equation (3.4) has an invariant density (which is reached exponentially) in a number of cases. All that is needed is that trajectories of the deterministic system

$$\dot{y} = g(x,y)$$

with x frozen have trajectories that are eventually bounded (see, Bhattacharya[2]). In general, however, $\bar{p}^{\lambda}(x,y)$ is not explicitly the form (3.10): however, the results of Ventsel - Freidlin [13] allow us to make the following statements about $\bar{p}^{\lambda}(x,y)$ in the limit that $\lambda \downarrow 0$.

The invariant density $\bar{p}^{\lambda}(x,y)$ concentrates as $\lambda \downarrow 0$ near the stable ω-limit sets such as stable equilibrium points, stable closed orbits and the like. Moreover, some of the stable ω-limit sets are preferred to others, as in Section 3.2, 3.3, where $\bar{p}^{\lambda}(x,y)$ concentrated at the <u>global</u> minima of $S(x,y)$ rather than the <u>local</u> minima (each of which represents a stable critical point or orbit of the flow as the case may be). In fact, $\bar{p}^{\lambda}(x,y)$ concentrates in some sense, above the <u>most-stable</u> ω-limit sets. This statement can be made mathematically precise using ideas from optimal control (see, e.g. Fleming and Mitter [3]); but, this development will be presented elsewhere since it is not in the mainstream of our present development. We only include here an example for which the foregoing intuitive statements are illustrated:

<u>Example 3.6</u> (Hopf Bifurcation in the Constraint Equation)

Consider with $x \in \mathbb{R}$, $y \in \mathbb{R}^2$ and $g(x,y)$ given by

$$\left.\begin{aligned} g_1(x,y) &= y_2 - y_1^3 + xy_1 \\ g_2(x,y) &= -y_1 \end{aligned}\right\} \tag{3.32}$$

Consider, just the sped up deterministic system with x fixed. For $x \leq 0$; its ω-limit set is a single stable equilibrium point at $y_1 = y_2 = 0$. For $x > 0$, a stable limit cycle initially approximately circular and of radius $0(\sqrt{x})$ emerges by the supercritical Hopf bifurcation (see e.g. Mees and Chua [8], Marsden, McCracken [7]) and the equilibrium point at $y_1 = y_2 = 0$ becomes unstable, as shown in Figure 9.

Clearly, then, the theory of Section 2 is no longer applicable. However, it is possible to show that as $\lambda \downarrow 0$, $\bar{p}^{\lambda}(x,y)$ concentrates on $y_1 = 0 = y_2$ for $x \leq 0$ and on the limit cycle $J(x)$ in the $y_1 - y_2$ plane for $x > 0$. The

limit distribution $\bar{p}^{\lambda}(x,y)$ on the limit cycle $J(x)$ is not uniform but is, as expected, inversely proportional to the magnitude of $g(x,y)$, at that point. (Intuitively, portions of $J(x)$ that are traversed more slowly are more likely). Thus, the limiting x-process satisfies

$$\dot{x} = f(x,0) \quad \text{for} \quad x \leq 0$$

and

$$\dot{x} = \frac{\oint_{J(x)} f(x,y) \frac{1}{||g(x,y)||} \, d\ell}{\oint_{J(x)} \frac{1}{||g(x,y)||} \, d\ell} \quad \text{for } x > 0 \qquad (3.33)$$

In (3.33) above all $d\ell$ is a segment of the orbit $J(x)$ □

Throughout the development so far we have assumed that the driving noise was state independent and non-degenerate, i.e. noise enters each of the y-equations. It has been pointed by Landauer [6], that the case of state dependent noise is extremely important in applications to the thermodynamics and in that instance the qualitative conclusions of Sections 3.2, 3.3 are changed. The case of state dependent noise will be treated elsewhere using the ideas of Fleming-Mitter [3], Ventsel-Freidlin [13]. However, the case of degenerate driving noise is one for which this author knows of no specific techniques of analysis. We will now point out an example in which $\bar{p}^{\lambda}(x,y)$ for an important class of constraint equations with degenerate driving noise can be obtained by ad-hoc means.

Example 3.7 (Constraint Equation of the Langevin form with degenerate driving noise).

Consider with $x \in \mathbb{R}^n$, $y = (y_1, y_2) \in \mathbb{R}^{n+m}$

$$\left.\begin{aligned} \varepsilon\dot{x} &= f(x,y) + \sqrt{\mu}\,\xi \\ \varepsilon\dot{y}_1 &= y_2 \\ \varepsilon\dot{y}_2 &= -y_2 + \operatorname{grad}_{y_1} V(x,y_1) + \sqrt{\varepsilon\lambda}\,\eta \end{aligned}\right\} \tag{3.34}$$

The sped-up system of (3.34) with x-fixed models the dynamics of a second order system with damping in a potential field described by $\operatorname{grad}_{y_1} V(x,y_1)$ and subject to fluctuations (called the Langevin model). It is easy to verify that if the derivatives with respect to y of V(x,y) go to ∞ sufficiently rapidly as $y \to \infty$ that $\bar{p}^{\lambda}(x,y)$ is of the form

$$K(x)\ \exp -\frac{1}{\lambda}\left(\frac{|y_2|^2}{2} + V(x,y_1)\right) \tag{3.35}$$

As before K(x) is chosen to normalize $\bar{p}^{\lambda}(x,y)$; now (3.35) is of the form studied in Sections (3.2), 3.3) so that the analysis of those sections applies for the limit as $\lambda \downarrow 0$ of $\bar{p}^{\lambda}(x,y)$.

One would guess the form (3.35)) for the invariant density of (3.34) since $\frac{1}{2}|y_2|^2 + V(x,y_1)$ is the 'natural' Lyaponov function (stored energy) for the deterministic fast system!

□

Section 4. The Effects of Thermal Noise on an Emitter-Coupled Relaxation Oscillator

We study in this section the relevance of the theory developed in Sections 2 and 3 to the study of the efeects of thermal noise on a relaxation oscillator. Figure 9 shows a simplified, circuit diagram of such an oscillator (the Analog Devices AD 537). We discuss first using the terminology of Section 2 the deterministic description of the oscillator: The circuit equations are given by

$$\frac{d}{dt}(V_{e2} - V_{e1}) = \frac{1}{C}(I_0 - i) \tag{4.1}$$

$$V_{b2} = V_{c1} = V_{cc} - iR \tag{4.2}$$

$$V_{b1} = V_{c2} = V_{cc} - (2I_0 - i)R \tag{4.3}$$

$$V_{bei} := V_{b1} - V_{e1} = V_T \ln \frac{i}{I_s} \tag{4.4}$$

$$V_{be2} := V_{b2} - V_{e2} = V_T \ln \frac{2I_0 - i}{I_S} \tag{4.5}$$

Here $V_T := \frac{kT}{q}$ is the threshold voltage for the base emitter junction and I_s is the reverse saturation current. The transistors are assumed to be identical. With $V := V_{e2} - V_{e1}$, we may combine equations (4.2) - (4.5) to obtain

$$\frac{d}{dt} V = \frac{1}{C}(I_0 - i) \tag{4.6}$$

$$0 = V - (2I_0 - 2i)R - V_T \ln \frac{2I_0 - i}{i} \tag{4.7}$$

Equations (4.6), (4.7) form an implicity defined dynamical system. The solution curve to the algebraic equation (4.7) is plotted in the (v,i)

plane in Figure 10. Some of the features of this curve are noted below:

(i) For $-2I_0R < V < 2I_0R$ the equation (4.7) has three solutions, while for $V > 2I_0R$ and $V < 2I_0R$ the equation has only one solution.

(ii) As $V \to \infty$, $i \to 2I_0$ and as $V \to -\infty$, $i \to 0$ asymptotically.

(iii) The values $V \cong 2I_0R$; $i \cong \frac{V_T}{2R}$ and $V \cong -2I_0R$, $i \cong 2I_0 - \frac{V_T}{2R}$ are the points of bifurcation of equation (4.7) with V treated as the bifurcation parameter, i.e. at these points it is not possible to solve (4.7) for i as a function of V locally and uniquely. These points may be shown to be points of fold bifurcation.

Returning now to the full system - (4.6) and (4.7) we see that continuous solutions for the system exist so long as i can be solved continuously as a function of v in (4.7) so as to obtain:

$$\frac{dv}{dt} = \frac{I_0 - i}{C} \tag{4.6}$$

and

$$\frac{di}{dt} = \frac{(I_0 - i)/C}{[-2R + V_T \cdot 2I_0/(2I_0 - i)i]} \tag{4.8}$$

When $-2R + V_T \cdot 2I_0/(2I_0 - i)i = 0$, i.e. $i = V_T/2R$ or $i = 2I_0 - V_T/2R$ it appears that $\frac{di}{dt}$ is infinite so as to prevent the integration of equations (4.6), (4.8). The regularization of this system is accomplished by taking into account the fact that parasitic capacitances present in the transistors, as well as the finite slew rate of the operational amplifiers will prevent i from varying discontinuously and in effect change the description of the

of the circuit dynamics from (4.6), (4.7) to

$$\frac{dV}{dt} = \frac{(I_0 - i)}{C} \tag{4.6}$$

$$\varepsilon \frac{di}{dt} = V - (2I_0 - 2i)R - V_T \ln(2I_0 - i)/i \tag{4.9}$$

Equations (4.6) and (4.9) are a gross simplification of all the actual parasitics present in the circuit. A more detailed and exhaustive description involving all the parasitics would start from the original equations (4.1) - (4.5). The present regularized model is, however, accurate enough for our purposes. The phase portrait of this system shown in Figure 1 includes a single unstable equilibrium point ($V=0$, $i=I_0$) and a limit cycle. The limit trajectories of (4.6), (4.9) as $\varepsilon \downarrow 0$ exist and include the relaxation oscillation shown in Figure 12 - a limit cycle with two discontinuities - at the points where the trajectory switches from the Q1 on, Q2 off 'state' to the Q1 off, Q2 on 'state' and vice versa. Note also from Figure 11 that the Q1 on, Q2 on 'state' is unstable as evidenced by the trajectories of (4.6), (4.9) pointing away from that 'state'. The current waveform $i(t)$ is as shown in Figure 13. The half period of the oscillation T may be estimated approximately by integrating equation 4.8 with the approximation that for $0 \leq t \leq T, i \ll I_0$, so that we have

$$T \cong \frac{C}{I_0} \int_{I_1}^{V_T/2R} (-2R + \frac{V_T}{i})\, di$$

or

$$T \cong \frac{C}{I_0} [2R(-V_T/2R + I_1) + V_T \ln(V_T/2I_1R)] \tag{4.10}$$

From equation (4.10) it follows that the frequency of oscillation is (approximately) lienarly proportional to I_0, which enables this oscillation to be used as an electronically tunable oscillator (e.g. in a phase locked loop). In such applications, it is important to know the noise characteristics of the oscillator in response to resistive thermal noise. Experimental observations of Abidi [1] indicate that the actual (noisy) current waveform is as shown in Figure 14. Key features of this figure are as follows:

(a) the transitions or jumps appear to be noise free

(b) the noise superimposed on the deterministic waveform of Figure 13 appears to be small (low intensity) immediately following a jump and then appear to build in intensity.

We assume (see e.g.[14]) that all the noise sources in the circuit can be lumped into a single-noisy current source $i_n(t)$ shown dotted in Figure 9: $i_n(t)$ is assumed to be white with intensity λ(with λ small at room temperatures, since it is proportional to kT). It is easy to check that the equation (4.6) is now unchanged, while (4.7) changes to

$$0 = V - (2I_0 - 2i)R - V_T \ell n(2I_0 - i)/i + 2R\sqrt{\lambda}\, i_n(t) \qquad (4.11)$$

We regularize the system (4.6), (4.11) as before to obtain

$$\dot{V} = (I_0 - i)/C \qquad (4.6)$$

$$\varepsilon\dot{i} = V - (2I_0 - 2i)R - V_T \ell n(2I_0 - i)/i + 2R\sqrt{\varepsilon\lambda}\, i_n(t) \qquad (4.12)$$

Note that ε scales the intensity of the white noise in (4.12) precisely for the same reason as in equation (3.2) of Section 3. The techniques of Section 3.2 may now be used to obtain that as $\varepsilon \downarrow 0$, the V-process converges weakly on $C([0,T]; \mathbb{R})$ to one satisfying :

$$\dot{V} = (I_0 - \bar{i}^{\lambda}(V))/C$$

where $\bar{i}^{\lambda}(v)$ is i integrated over the conditional density for i given V,in the limit that $\varepsilon \downarrow 0$, $\bar{p}^{\lambda}(i,v)$. As in the example of Section 3.2, we have in the limit that $\lambda \downarrow 0$, $\bar{p}^{\lambda}(i,v)$ converging to a sequence of delta functions jumping from one leg of the solution curve to (4.7) to the other at $V=0$. Also, choosing the interval of weak convergence to be large it appears that the relaxation oscillation is borken up.

This analysis is contrary to the experimental evidence of Abidi [1] What has gone wrong? How does one recover the experimental results of Abidi [1]? These are the questions that we taken up next.

Section 5. Sample Function Calculations.

The mathematical reason for the anomaly between the machinery developed in Section 3 and the experimental conclusions of Section 4, is the order of limits $\varepsilon \downarrow 0$ followed by $\lambda \downarrow 0$ in Theorem (3.3). This order of taking limits is suitable for explaining phenomena in several situations in non-equilibrium thermodynamics (for e.g. phase transitions of the kind discussed in Sastry-Hijab [12], Eyring chemical reaction rates, etc. - see for e.g. Nicolis-Prigogine [9], Landauer [6]). In fact, it has been noted by thermodynamicists of the Brussels School that "fluctuations play a crucial role in changing the behavior of systems near bifurcation fronts". However, this order of limits is not fully satisfactory in the circuit context. The reason for this lies in the fact that the order of limits $\varepsilon \downarrow 0$ followed by $\lambda \downarrow 0$ (Theorem 3.3) yields the correct conclusions only when the dynamics of the fast (sped-up) system are much faster than those of the slower x variable. This is so, because, as we state in Section 3.4, Laplace's method of steepest descent picks for the limit values of $\bar{p}^{\lambda}(x,y)$ as $\lambda \downarrow 0$ the most stable ω-limit sets of the underlying deterministic systems. This in turn is consistent with the intuition that in the presence of persistent random perturbation (wide-band in nature) the trajectories of a system will concentrate after sufficiently long periods of time in the vicinity of the most-stable sets. However, the sufficiently long periods of time may be very large indeed. It is possible to show, for example in the gradient case of Section 3.2 that the average time required to excape from a stable equilibrium is of the order of $e^{k/\lambda}$ for some $k>0$ (see for eg. Schuss [15], Ventsel-Freidlin (15]).

By taking limits in the sequence $\varepsilon \downarrow 0$ follower by $\lambda \downarrow 0$, the implication is that ε is smaller than $e^{-k/\lambda}$, i.e. ε is at least $o(e^{-k/\lambda})$, so that the fast system has sufficiently much time to concentrate in the vicinity of its ω-limit sets. This is frequently the situation in non-equilibrium theromodynamics where the slower dynamics are frequently assumed to be 'quasi-static'. In the circuit context, however, the separation of time scales between the slow and fast variable is not as large as is implied by the theorem.

As noted in the remark following Theorem 3.3; if the order of limits is interchanged (i.e. $\lambda \downarrow 0$ and then $\varepsilon \downarrow 0$), one recovers the deterministic development of Section 2. Before, we further elaborate and make precise the statements of the previous paragraph we indicate how one analyses sample functions of the process generated by (3.1), (3.2) in the limit that $\lambda \downarrow 0$ followed by $\varepsilon \downarrow 0$. The major tool for this development is the work of Ventsel-Freidlin [13].

We consider here sample functions of the process generated by

$$\dot{x} = f(x,y) + \sqrt{\lambda}\,\xi, \qquad x(0) = x_0 \tag{5.1}$$

$$\varepsilon\dot{y} = f(x,y) + \sqrt{\lambda\,\varepsilon}\,\eta \qquad y(0) = y_0 \ . \tag{5.2}$$

with precisely the same assumptions as in Section 3. Let $\psi = [\psi_x, \psi_y]$: $[0,T] \to \mathbb{R}^n \times \mathbb{R}^m$ be a C^1 map from the interval $[0,T]$ to the x, y space with $\psi_x(0) = x_0$, $\psi_y(0) = y_0$. Define, for this trajectory, the functional $I_\varepsilon(\psi)$ by

$$I_\varepsilon(\psi) = \int_0^T \left\| \begin{matrix} \dot{\psi}_x(t) - f(\psi_x, \psi_y) \\ \varepsilon[\dot{\psi}_y(t) - \frac{1}{\varepsilon} g(\psi_x, \psi_y)] \end{matrix} \right\|^2 dt \ . \tag{5.3}$$

Then, we have the following theorem for measuring the derivation of the sample functions of (5.1), (5.2) from the (arbitrarily specified) trajectory ψ.

Theorem 5.1 [13]

For any $\delta, h > 0$ there eixsts a $\lambda_0 > 0$ such that

$$\text{Prob}\left\{ \sup_{t\in[0,T]} \left|\left| \begin{matrix} \psi_x(t) - x(t) \\ \psi_y(t) - y(t) \end{matrix} \right|\right| < \delta \right\} > \exp - \frac{I_\varepsilon(\psi) + h}{2\lambda} \qquad (5.4)$$

Remarks: (1) Equation (5.4) gives an estimate of how close the sample functions of the process of (5.1), (5.2) lie to the arbitrarily specified $\psi:[0,T] \to \mathbb{R}^n \times \mathbb{R}^m$. Clearly, the estimate (5.4) is sharpest when its right hand side is as close to 1 as possible, i.e. when ψ is chosen to minimize $I_\varepsilon(\psi)$. We examine this point next.

(2) Consider the definition of $I_\varepsilon(\psi)$ in equation (5.3). Note that if $\psi:[0,T] \to \mathbb{R}^n$ is, in fact, the solution trajectory of the deterministic system starting from (x_0, y_0); then $I_\varepsilon(\psi) = 0$, its minimum value. Further (5.3) is, for arbitrary ψ, a measure of how far ψ fails to satisfy the flow of the deterministic system.

(3) Note the ε weighting on the y-component of equation 5.3. Taking the limit that $\varepsilon \downarrow 0$; we see that so long as $\dot{\psi}_y$ remains bounded the contribution of the second term is merely $||g(\psi_x, \psi_y)||^2$.

(4) Note that Theorem 5.1 gives an estimate for the deviation of the process of (5.1), (5.2) from the trajectory ψ for fixed ε and $\lambda \downarrow 0$ as follows: For $\varepsilon > 0$ with probability arbitrarily close to 1, the most likely trajectory for the process is that which minimizes $I_\varepsilon(\psi)$. Further, taking the limit that

that $\varepsilon \downarrow 0$ and allowing for trajectories ψ that are no longer differentiable in y and piecewise differentiable in x, it is clear that when a solution to $g(\psi_x, \psi_y) = 0$, $\dot{\psi}_x = f(\psi_x, \psi_y)$ exists this is the solution minimizing $I_0(\psi)$. Further, a jump from (x_0, y_0) to (x_0, y_1) is permissible for the minimizing $I_0(\psi)$ if there exists a trajectory starting arbitrarily close to y_0 and following the integral curve of

$$\dot{y} = g(x_0, y)$$

to y_1. This is precisely the case when y_0 is unstable and belongs to the boundary of the domain of attraction of y_1. As in the development of Section 2 several jumps may be permissible from y_0 to y_1, y_2, etc. as shown in Figure 16. Thus, in such cases there may be several trajectories ψ which minimize $I_0(\psi)$. Theorem (5.1), only predicts that the sample path of the process will be an a δ-neighborhood of one of them. A similar difficulty arises at points of bifurcation of $g(x,y)$.

Another useful estimate is also given in [15]: Define Φ_0 to be the set of C^1 functions $\psi(x,y)$ defined from $[0,T] \to \mathbb{R}^n x \mathbb{R}^m$ such that $I_\varepsilon(\psi) \leq I_0$. Then, we have

Theorem 5.2 [15]

For any $\alpha>0$, $\delta>0$, there exists a λ_0 such that

$$\text{Prob}\left\{\text{dist}\left(\begin{pmatrix} x(t) \\ y(t) \end{pmatrix}, \Phi_0\right) \geq \delta\right\} \leq 2\exp \frac{-(1-\alpha)I_0 + \alpha T}{2\lambda} \tag{5.5}$$

for all $\lambda \leq \lambda_0$, where

$$\text{dist}\left(\begin{pmatrix} x(t) \\ y(t) \end{pmatrix}, \Phi_0\right) = \inf_{\psi \in \Phi_0} \sup_{t \in [0,T]} \left|\left| \begin{matrix} \psi_x(t) - x(t) \\ \psi_y(t) - y(t) \end{matrix} \right|\right|$$

is the distance between the sample function and the set Φ_0.

Remarks:

(1) By choosing I_0 so as to make the quantity on the right hand side small; we can guarantee that the sample functions of the process of (5.1), (5.2) are close to Φ_0.

(2) The drawback of Theorem (5.2) is that the set Φ_0 is generally an extremely badly behaved set; since $I_\varepsilon(\psi)$ is an integral criterion.

(3) While theorem (5.2) cannot be applied in its present form to explain the experimental conclusions of Section 4, the following heuristic explanation can now be given for the sample function of Figure 15:

As the trajectory ψ nears the points of jump i.e. $V = \pm 2I_0R$; it can admit larger and larger derivations in V and i (as may be verified graphically, see Figure 17) for the same increase in the right hand side of (4.9) which figures in $I_\varepsilon(\psi)$ of (5.3). Thus, the set Φ_0 includes trajectories which lie inside the tube shown in Figure 17. Note that the tube is thicker near the points of jump so that trajectories which appear to be more noisy around the jump points are allowable. Note that the jumps themselves appear to be noise free because of the fact that these represent dynamics with the time compressed by a factor of $1/\varepsilon$.

Section 6. Conclusions

We have analyzed in this paper the effect of the addition of small-noise to an implicitly defined non-linear dynamical system. The implicitly defined dynamics are regularized in Section 2 by augmenting the dynamics with 'fast' dynamics. Depending on the relative separation between the time scales of the slow and fast dynamics of the regularized system and the noise intensity two kinds of results have been derived.

In Section 3, it is assumed that the separation in time scales is more significant that the intensity of the white noise (characterized by the sequence of limits $\varepsilon \downarrow 0$ followed by $\lambda \downarrow 0$). The resulting equations are of relevance to the study of the dynamics of phase transitions, reaction rates and other topics of non-equilibrium thermodynamics. In Section 4, we show that the conclusions of Section 3 are not relevant to the study of the noise behavior of non-linear circuits, in particular, a multivibrator. This is because the separation of time scales between parasitic and non-parasitic circuit elements is not very large. In Section 5, we introduce new machinery to study the system dynamics when the small intensity of the noise is more significant than the separation of time scales (characterized by the sequence of limits $\varepsilon \downarrow 0$ followed by $\lambda \downarrow 0$).

The present paper presents the first step in developing a comprehensive and useful theory of the dynamics of implicit systems driven by white noises. It is a first step in understanding the noise behavior of non-linear circuits - a topic of great importance in the simulation of VLSI circuits particularly as devices shrink in size.

References

[1] Abidi, A.A., "Effects of Random and Periodic Excitations on Relaxation Oscillations", ERL Memo No. M81/80, University of California, Berkeley, Sept. 1981.

[2] Bhattacharya, R.N., "Criteria for Recurrence and Existence of Invariant Measures for Multidimensional Diffusions", The Annals of Probability, Vol. 6 (1978) pp. 541 - 553.

[3] Fleming, W.H. and Mitter, S.K., "Optimal Control and Non-linear Filtering for Nondegenerate Diffusions", M.I.T., L.I.D.S., Preprint, Sept. 1981.

[4] Hale, J.K., "Generic Bifurcation with Applications", in Non-linear Analysis and Mechanics - the Heriot Watt Symposium, Vol.I, Pitman, 1977, pp. 59 - 157.

[5] Hijab, O., "Minimum Energy Estimation", Ph.D. dissertation, University of California, Berkeley, Dec. 1980.

[6] Landauer, R., "The Role of Fluctuations in Multistable Systems and in the Transition to Multistability", in Bifurcation Theory and Applications in Scientific Disciplines, O. Gurel and O.E. Roessler, editors, N.Y. Academy of Sciences, 1979, pp. 433.

[7] Marsden, J.E. and McCracken, M., "The Hopf Bifurcation and its Applications", Springer Verlag, Applied Math. Science Series, Vol. 19, (1976).

[8] Mees, A.I. and Chua, L.O., "The Hopf Bifurcation and its Application to Non-linear Oscillations in Circuits and Systems", IEEE Trans. on Circuits and Systems, Vol. CAS-26 (1979) pp. 235-254.

[9] G. Nicolis and I. Prigogine, "Self Organization in Non Equilibrium Systems", Wiley (New York), 1977

[10] Papanicolaou, G.C., Stroock, D. and Varadhan, S.R.S., "Martingale Approach to Some Limit Theorems" in Statistical Mechanics, Dynamical Systems and the Duke Turbulence Conference, ed.D. Ruelle, Duke Univ. Math. Series, Vol. 3, (1977).

[11] Sastry, S.S. and C.A. Desoer, "Jump Behavior of Circuits and Systems", IEEE Trans. on Circuits and Systems, Vol. CAS-28 (1981) pp. 1109 - 1124.

[12] Sastry, S.S. and O. Hijab, "Bifurcation in the Presence of Small Noise", Systems and Control Letters, Vol. 1, (1981), pp. 159-166.

[13] Ventsel, A.D. and Freidlin, M.I., "On Small Random Perturbations of Dynamical Systems", Upsekhi Mathematika Nauk, Vol.25 (1970) pp. 3-55.

[14] Meyer, R.G. Nonlinear Analog Integrated Circuits, EE 240 class notes at Univ. of California, Berkeley, 1976 (to be published).

[15] Schuss, Z., Theory and Applications of Stochastic Differential Equations, John Wiley, 1980, esp. Chapters 7 and 8.

[16] Milnor, J., Morse Theory, Annals of Mathematics Studies, Princeton University Press, 1973.

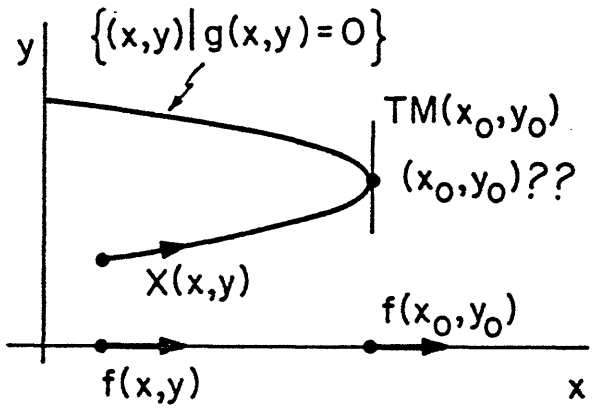

Figure 1: Illustrating the Difficulties in Obtaining X(x,y) from f(x,y)

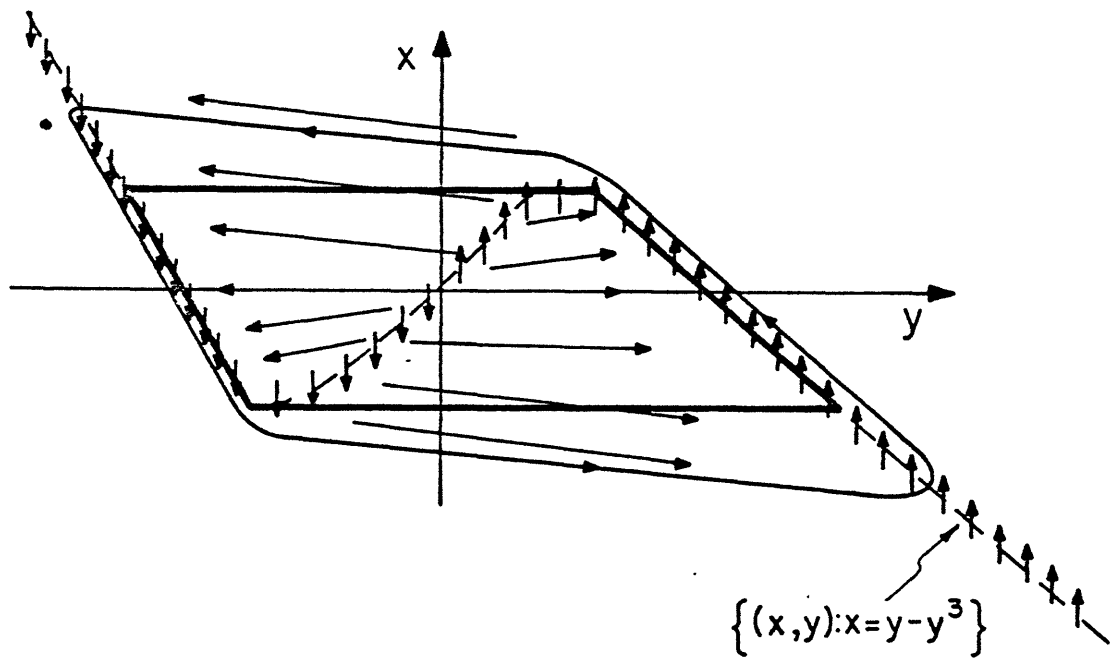

Figure 2: Showing the dynamics of the Degenerate and Regularized van der Pol Oscillator

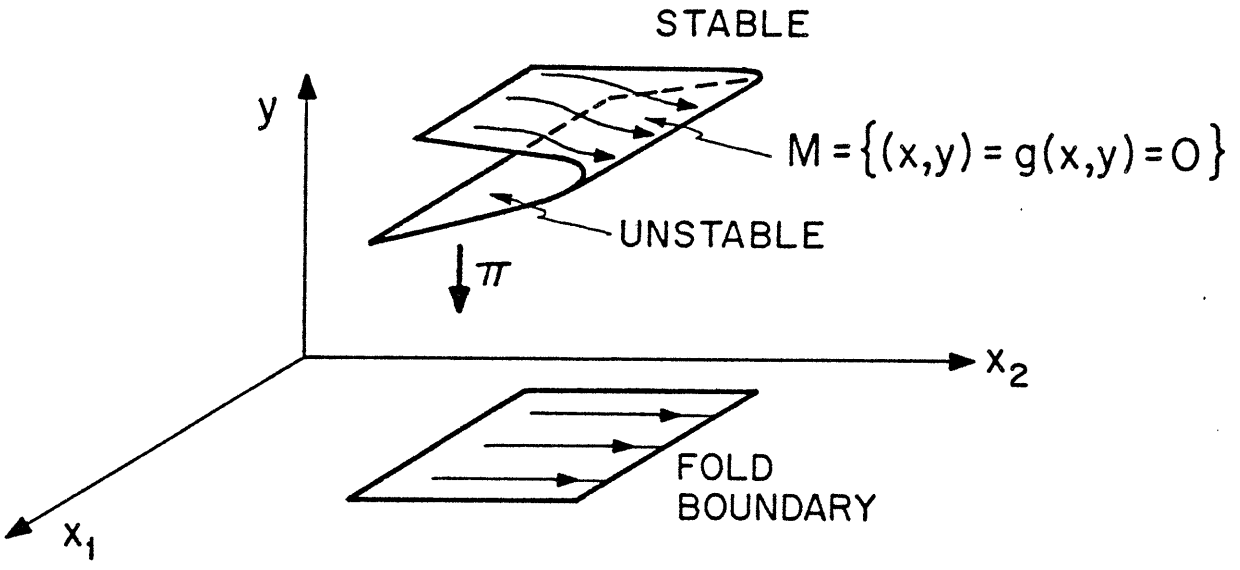

Figure 3: Visualizing a Fold Bifurcation and the Trajectories on M Pointing Towards the Fold Boundary

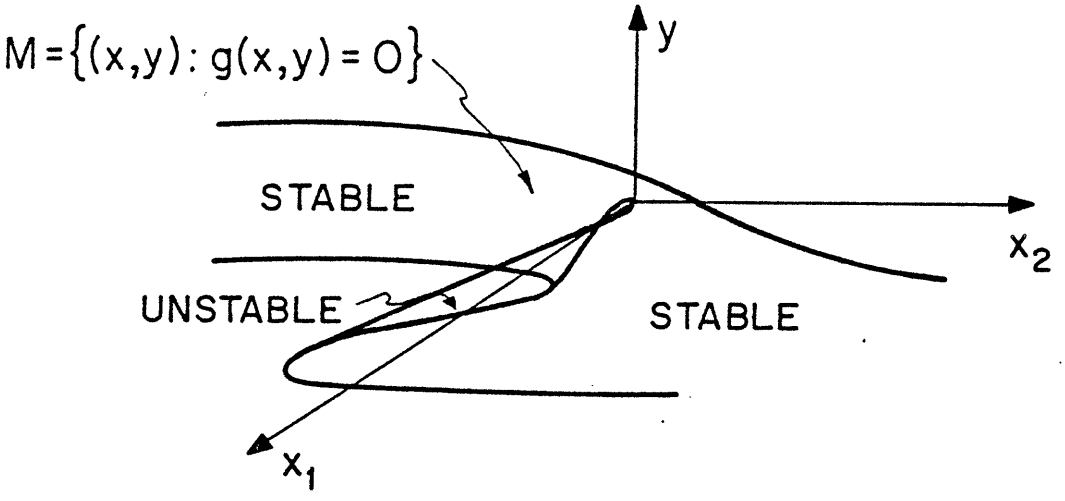

Figure 4: Visualization of a Cusp Bifurcation

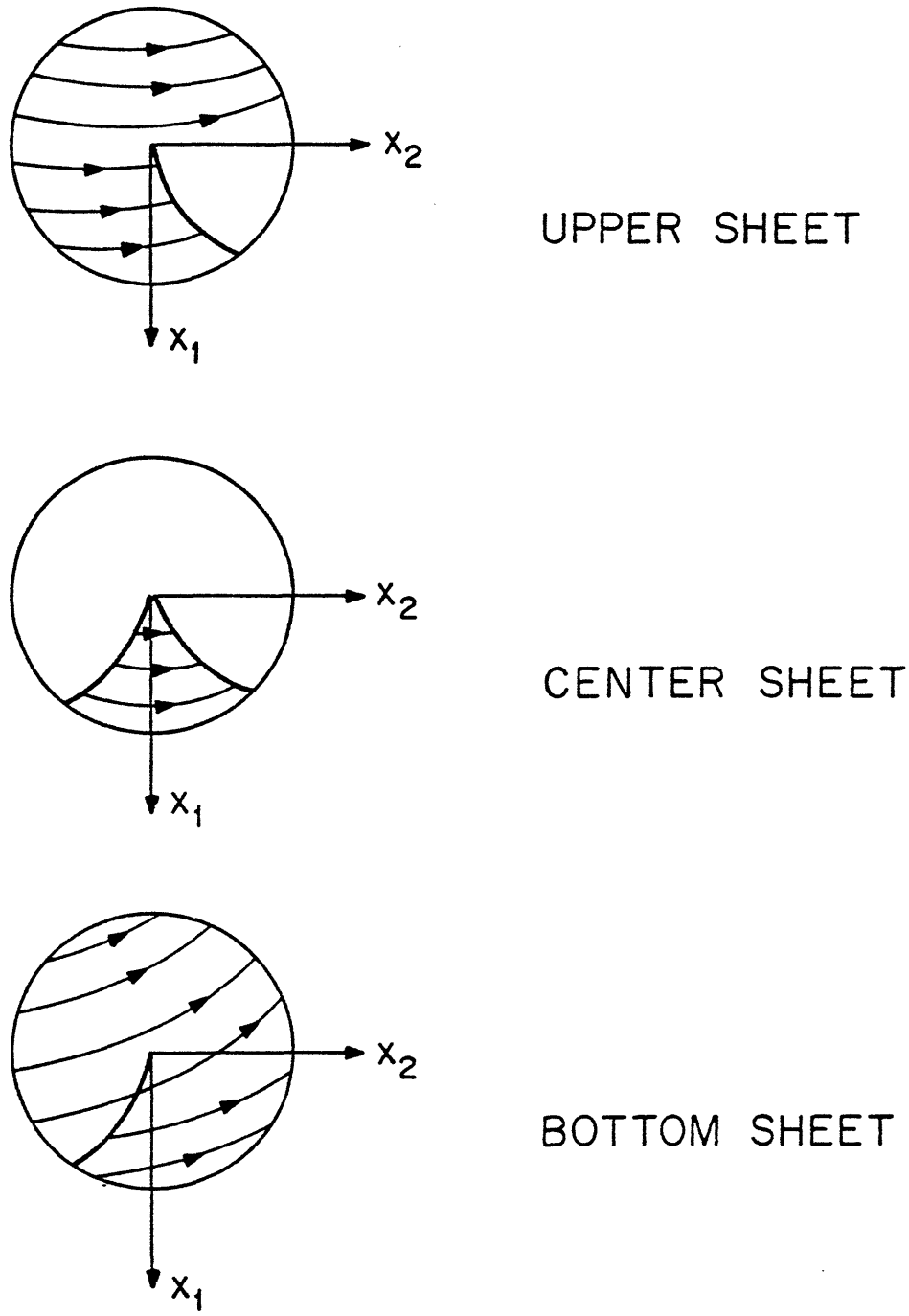

Figure 5: Visualization of the Trajectories on the Upper, Center and Bottom Sheets of the Cusp

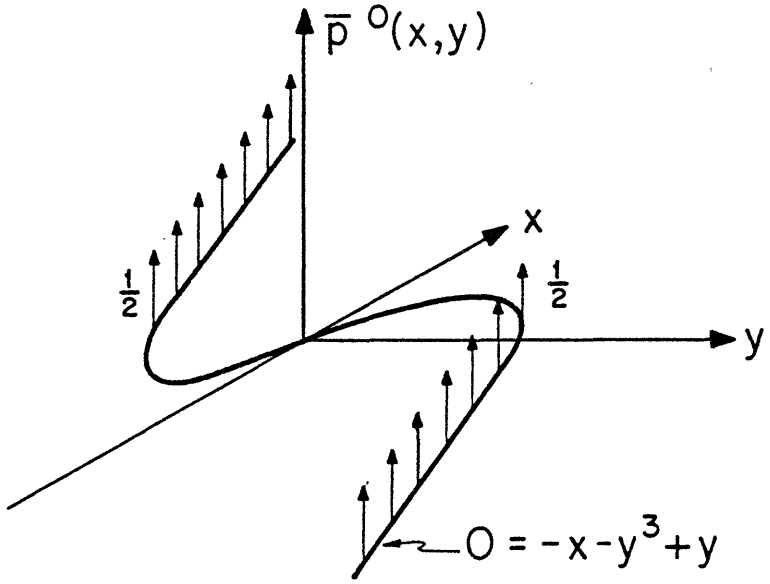

Figure 6: Showing the Limit as $\lambda \downarrow 0$ of the Conditional Density $\bar{p}^{\lambda}(x,y)$

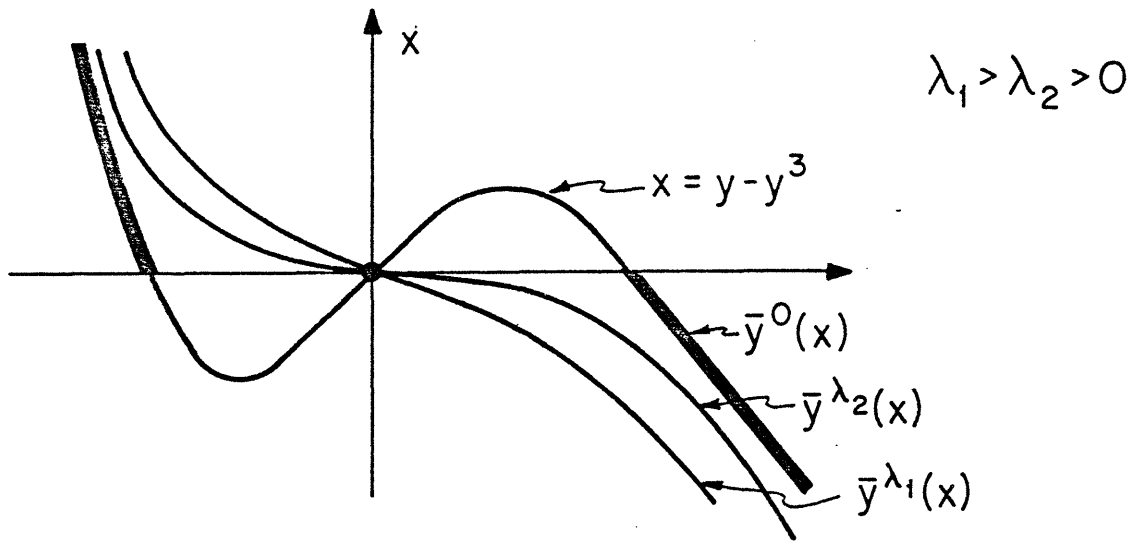

Figure 7: The Drift $\bar{y}^{\lambda}(x)$ for the Limit Diffusion of the van del Pol Oscillator for Decreasing Values of λ .

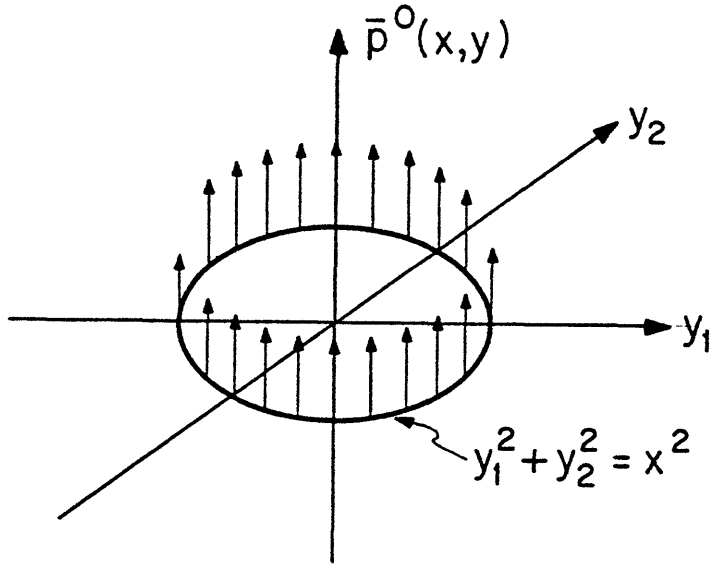

Figure 8: Showing the Limit Behavior of $\bar{p}^{\lambda}(x,y)$ for Example 3.5

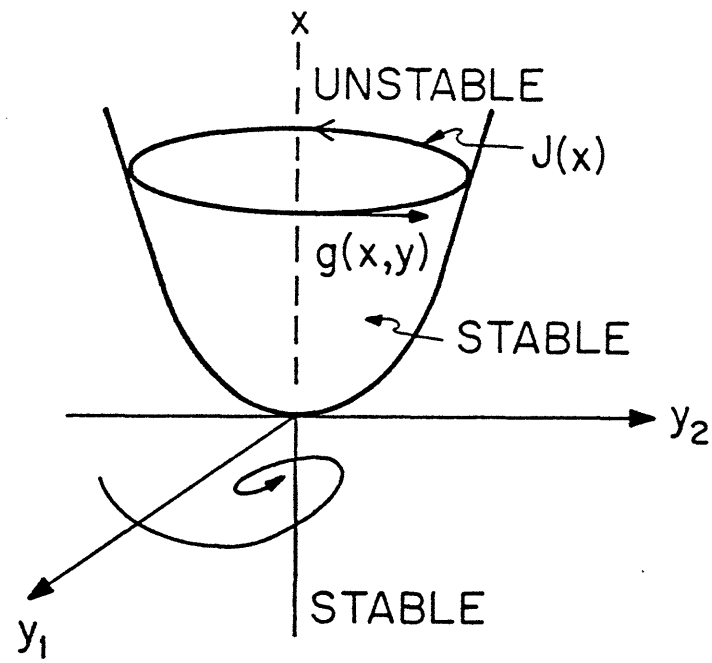

Figure 9: Showing the Hopf Befurcation for the Example 3.6

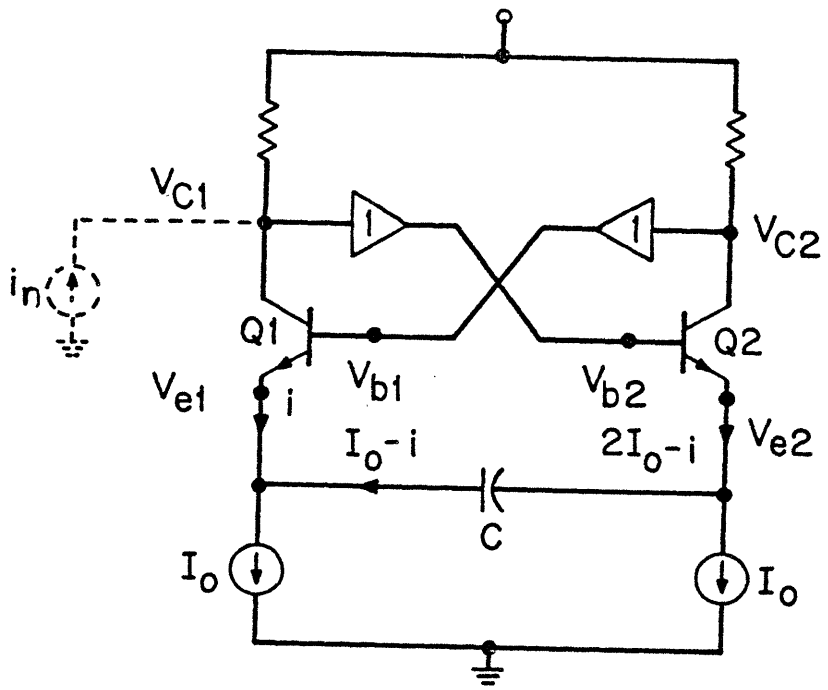

Figure 10: Simplified Circuit Diagram for the Emitter Coupled Relaxation Oscillator

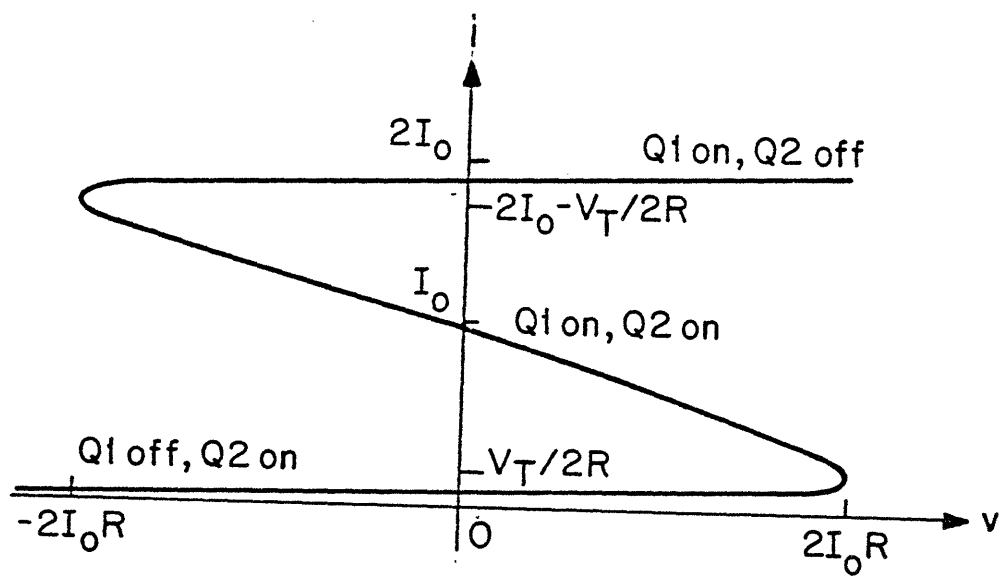

Figure 11: The Solution Curve to the Algebraic Equation (4.7)

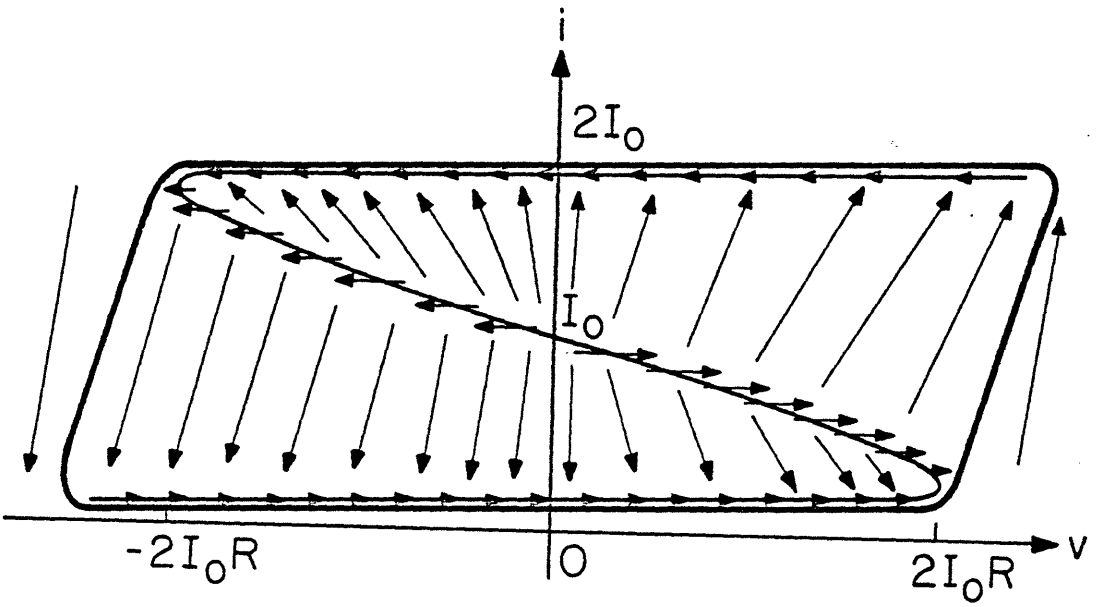

Figure 12: Phase Portrait of the System (4.6) , (4.9)

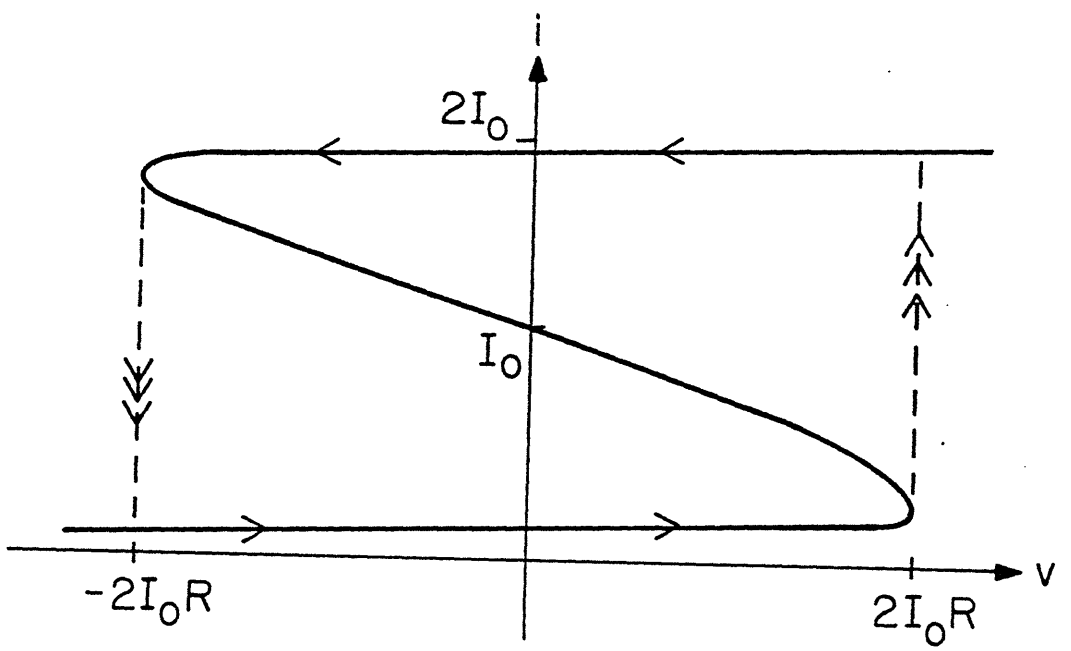

Figure 13: Showing the Relaxation Oscillation in the Emitter Coupled Oscillator

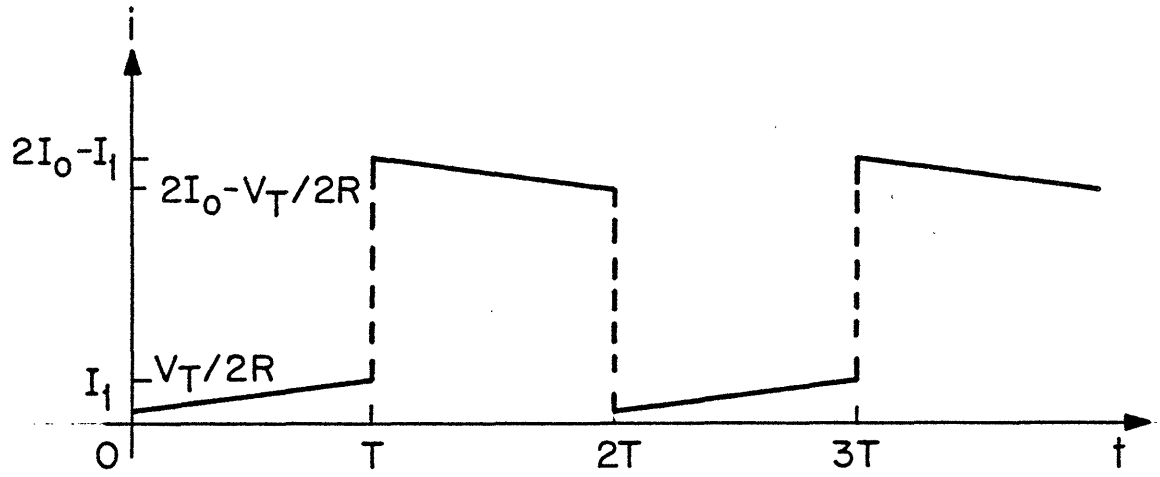

Figure 14: Current Waveform i(t) for the Circuit of Figure 1.

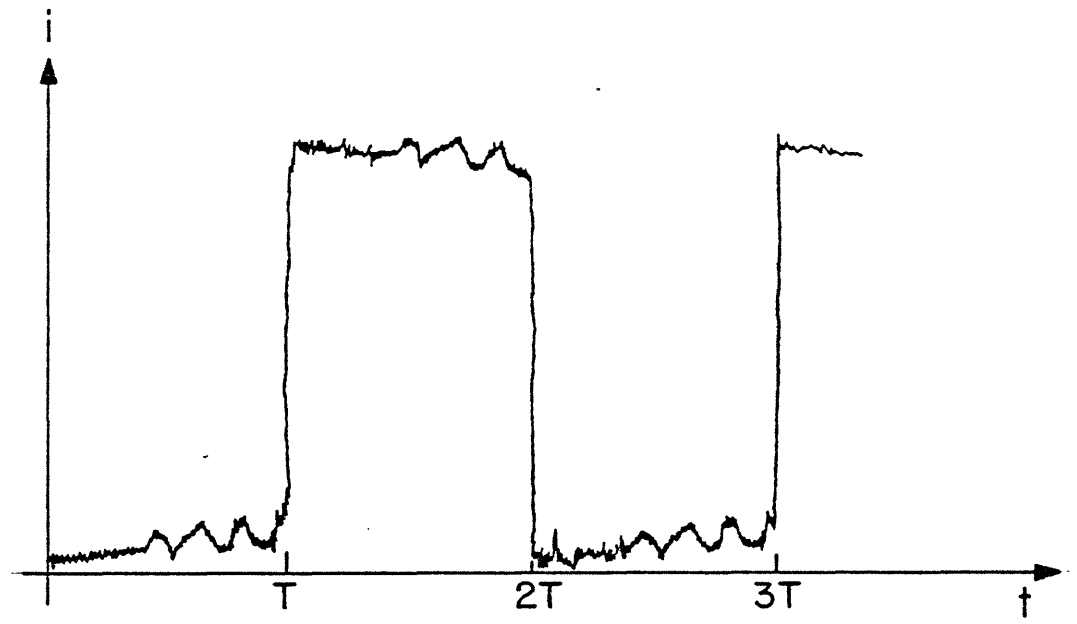

Figure 15: Experimentally Observed Waveform for i(t) in the Presence of Noise (after Abidi[1])

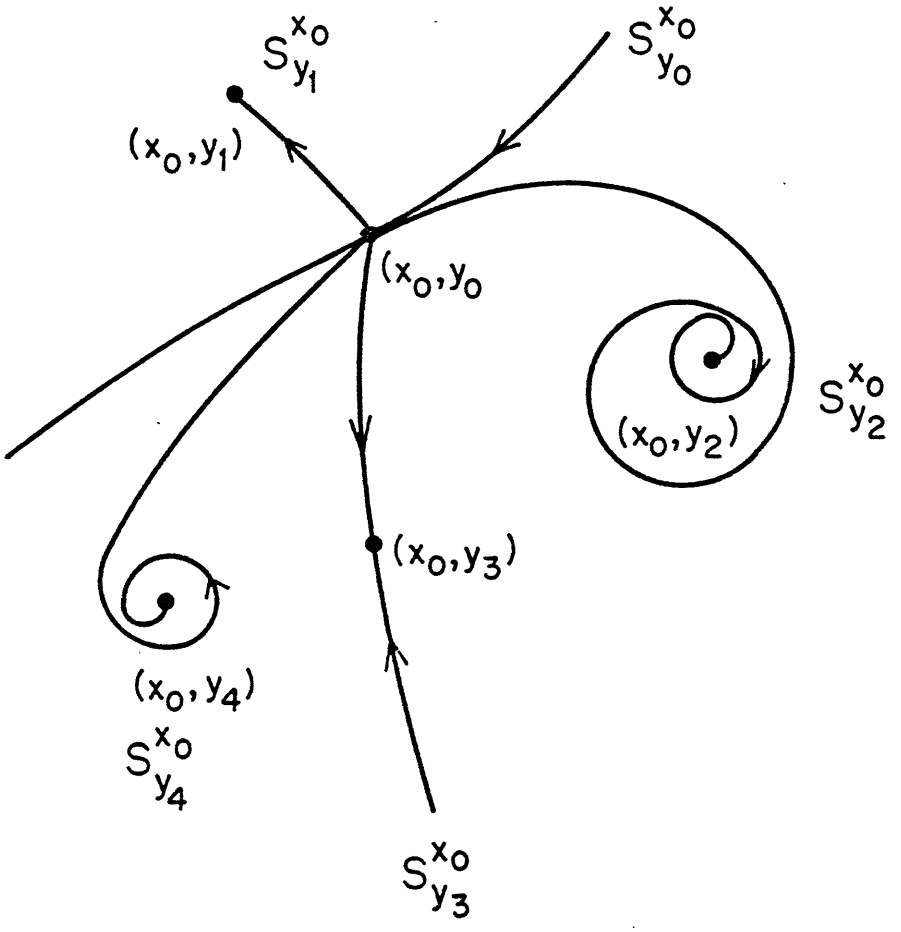

Figure 16: Showing the Possibility of jump from y_o to y_1, y_2, y_3 or y_4

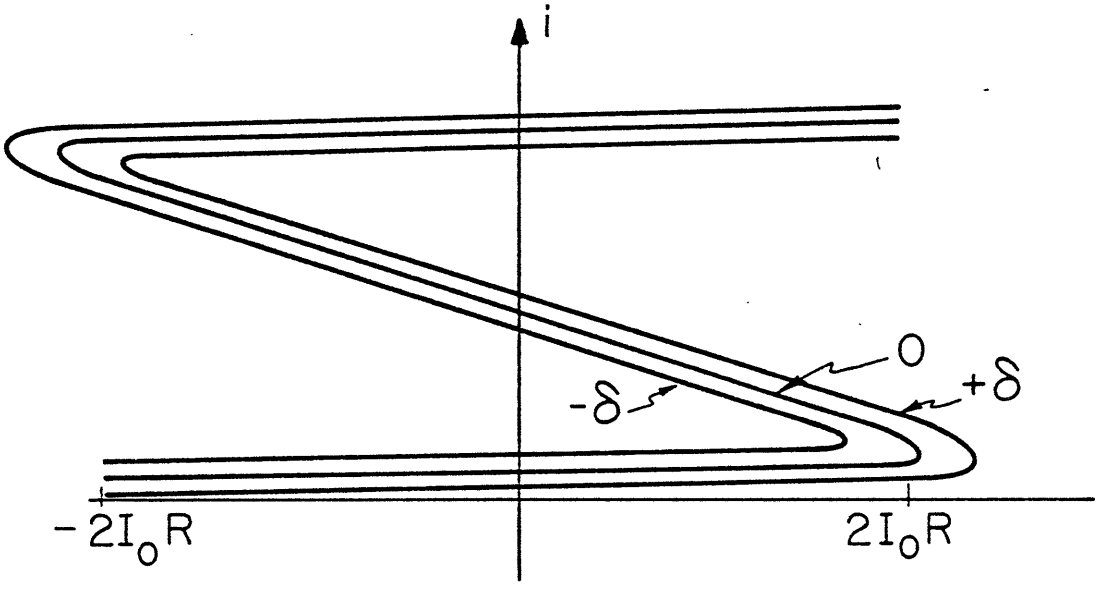

Figure 17: Showing a δ neighbourhood of the Constraint Equation (4.7)